

The dependence of spatial autoresonance in SRS on $k_L \lambda_D$

T. Chapman^{1,a}, S. Hüller¹, P.E. Masson-Laborde², A. Heron¹, W. Rozmus³
and D. Pesme¹

¹ *Centre de Physique Théorique, CNRS, Ecole Polytechnique, Palaiseau, France*

² *CEA, DAM, DIF, 91297 Arpajon*

³ *Theoretical Physics Institute, Department of Physics, University of Alberta, Edmonton, Canada*

Abstract. Spatial autoresonance is investigated as a mechanism for the enhancement of stimulated Raman scattering (SRS) in the kinetic regime ($k_L \lambda_D > 0.29$). Autoresonance in 3-wave simulations was demonstrated in a previous study [Chapman *et al.*, Phys. Plasmas **17**, 122317 (2010)]. These results are applied to particle-in-cell (PIC) simulations. Good agreement is found between PIC simulations and a 3-wave model using a nonlinear frequency shift beyond the regime usually referred to as “weakly kinetic”. Autoresonance is studied for a range of values of $k_L \lambda_D$.

1. INTRODUCTION

A nonlinear oscillator driven from rest at a fixed frequency will quickly dephase from its driver, ending the efficient exchange of energy. However, if the driver is instead swept in frequency, passing slowly through resonance with the oscillator, the oscillator may undergo *autoresonance*, phase-locking to the driver and remaining in resonance as its amplitude grows. During autoresonance, the oscillator self-adjusts its amplitude, and therefore frequency, in order to maintain resonance. This process may occur without feedback, and thus is applied in a range of contexts where the constraints on the speed and precision of driver modulation required to maintain resonance artificially would be unattainable: recent examples in plasmas include the control of the diocotron mode in a Malmberg-Penning trap [1], and the manipulation of anti-protons and positrons to form anti-hydrogen [2].

Stimulated Raman scattering is the 3-wave parametric instability in which laser light (the pump wave) scatters off of a density fluctuation in a plasma, driving a Langmuir wave. The scattered light (the seed wave) beats with the laser light, further enhancing the ponderomotive force that drives the Langmuir wave, leading to unstable growth. A range of processes may detune the 3-wave resonance necessary for the efficient scattering of the laser light. This article considers the interplay between two detuning mechanisms: the inhomogeneity of the plasma density profile, and kinetic effects.

The linear dispersion relations of the three waves are functions of the local electron plasma frequency, ω_{pe} . Consequently, as a given excited mode (electromagnetic or electrostatic) propagates, it undergoes a wave number shift. Three waves initially resonant at density n_0 , with pump, seed and Langmuir wave frequencies $\omega_{0,1,L}$ and wave numbers $k_{0,1,L}$, respectively, will dephase from resonance due to this wave number shift as they propagate through the changing density. At n_0 , the resonance conditions $\omega_0 = \omega_1 + \omega_L$ and $k_0 = k_1 + k_L$ are satisfied. The wave number shift $\kappa' \equiv \partial_x(k_0 - k_1 - k_L)$ is dominated by the Langmuir wave, thus in a linear density profile, $\kappa' \approx -\partial_x k_L = \omega_{pe}^2 / 6L v_{th}^2 k_L$ to

^ae-mail: chapman29@l1n1.gov

a good approximation [3], where v_{th} is the electron thermal velocity and L parameterises the density gradient such that $L = (1/n_0)(dn_e/dx)$, for which n_e is the local electron density. In a plasma of linear density profile and sufficient length to allow the convective growth to saturation of the waves, the growth of the Langmuir wave and scattered light was shown, in the absence of nonlinear processes, to be saturated by this wave number shift in a predictable fashion by Rosenbluth [4]: a seed wave of initial amplitude I_1 will be amplified to a level $I_1 \exp(2G_R)$, where G_R is the gain factor defined in Ref. [4].

As the amplitude of the Langmuir wave grows, electrons near the phase velocity may become trapped in the potential wells formed by the wave. The trapping alters the electron distribution function, resulting in a lower local Langmuir wave frequency. This nonlinear frequency shift $\delta\omega^{\text{nl}}$ was calculated by Morales and O'Neil to be of a form such that $\omega_L^{\text{nl}} = \omega_L - \delta\omega^{\text{nl}}$, $\delta\omega^{\text{nl}} = \eta|\varepsilon_L|^{1/2}$ [5], where ε_L is the longitudinal electric field envelope amplitude, η is a positive parameter and ω_L is the linear Langmuir wave frequency. Electron trapping may also greatly reduce the Landau damping present in the plasma [6]. Even the inversion of the electron distribution function around the phase velocity has been observed. The regime associated with this process, called ‘‘kinetic inflation’’ [7] is known to destabilise SRS, and has been investigated in homogeneous plasmas, leading to reflectivities far higher than those predicted by linear theory in the kinetic regime (the regime in which the dominant nonlinear processes are of kinetic origin), typically defined as corresponding to $k_L\lambda_D \gtrsim 0.29$ [8].

Under similar conditions to those adopted in this article, 1D and 2D particle-in-cell (PIC) simulations were performed by Masson-Laborde *et al.* [9, 10] which showed good agreement with a 3-wave coupling model using a nonlinear frequency shift, while the early behaviour of the plasma (up to the first saturation of the reflectivity) was found to be predominantly governed by 1D effects [9].

We consider here inhomogeneous plasmas, and restrict ourselves to a study in 1D, noting that AR is possible in higher dimensional problems [11], as discussed also in Ref. [10]. In the following section, a 3-wave coupling model is introduced (described in detail in Ref. [12]) that includes the effects of inhomogeneity and a kinetic nonlinear frequency shift, allowing autoresonance to be studied. This model is used to explain the results of PIC simulations where a single Langmuir wave mode is preferentially driven by using counter-propagating narrowband laser beams, allowing the unambiguous identification of autoresonance. These findings are then used to explain observations in PIC simulations where, complementary to previous work [10], only a single laser is applied to the plasma and SRS grows from the broadband noise present in the plasma.

2. THREE-WAVE COUPLING MODEL

We adopt an envelope description of the three waves, separating slowly- and quickly-varying phases. We write the 3-wave equations in the following form, relevant to an underdense warm inhomogeneous plasma in the weakly kinetic regime:

$$\mathcal{L}_0 A_0 = -\Gamma_0 A_1 \varepsilon_L, \quad (1)$$

$$\mathcal{L}_1 A_1 = \Gamma_1 A_0 \varepsilon_L^*, \quad (2)$$

$$(\mathcal{L}_L + i\kappa' c_L(x - x_r) - i\eta|\varepsilon_L|^{1/2}) \varepsilon_L = \Gamma_L A_0 A_1^*, \quad (3)$$

where the envelope amplitudes of the electromagnetic pump and seed potentials are given by $A_{0,1}$ and the coupling strengths by $\Gamma_{0,1} = ek_L/4m_e\omega_{0,1}$, $\Gamma_L = (ek_L/4m_e\omega_L)\omega_{pe}^2$, for which e and m_e are the electron charge and mass, respectively. The waves propagate through the operators $\mathcal{L}_{0,1,L} = \partial_t + c_{0,1,L}\partial_x$, where $c_{0,L} = \partial_k\omega_{0,L} > 0$, $c_1 = \partial_k\omega_1 < 0$ are the group velocities (since we wish to study the kinetic regime, we consider the case where laser light is scattered backwards). Landau damping is not included here in

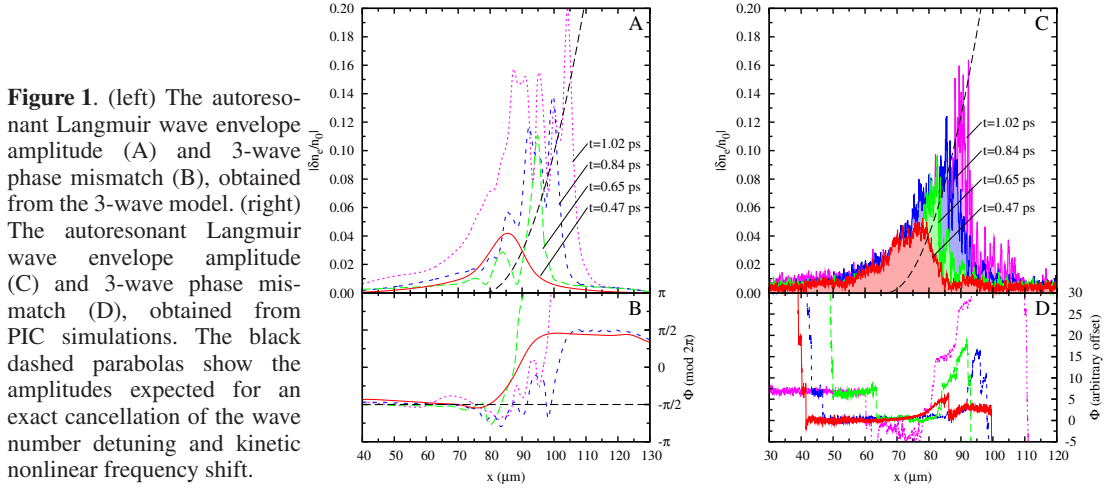


Figure 1. (left) The autoresonant Langmuir wave envelope amplitude (A) and 3-wave phase mismatch (B), obtained from the 3-wave model. (right) The autoresonant Langmuir wave envelope amplitude (C) and 3-wave phase mismatch (D), obtained from PIC simulations. The black dashed parabolas show the amplitudes expected for an exact cancellation of the wave number detuning and kinetic nonlinear frequency shift.

the equations due to the presence of kinetic effects, but is present in the 3-wave and PIC simulations discussed later.

The three waves are initially resonant at x_r in the plasma. The wave number detuning from resonance either side of x_r is described by the term $i\kappa'c_L(x - x_r)$ in Eq. (3). During autoresonance, the Langmuir wave self-adjusts its frequency through its amplitude via the term $i\eta|\varepsilon_L|^{1/2}$ in Eq. (3) in order to cancel the wave number detuning over a region in space. Beginning at x_r , as the Langmuir wave propagates in the direction $x > x_r$, the Langmuir wave amplitude would have to grow parabolically in space to maintain the cancellation. We therefore expect during autoresonance the following:

$$|\varepsilon_L| = \left(\frac{\kappa'c_L}{\eta}\right)^2 (x - x_r)^2 \quad \text{or} \quad \left|\frac{\delta n_e}{n_0}\right| = \left(\frac{\kappa'c_L}{\omega_L \tilde{\eta}}\right)^2 (x - x_r)^2, \quad (4)$$

where by Poisson's law $\eta = \omega_L(\epsilon_0 k_L/n_0 e)^{1/2} \tilde{\eta}$ and $|\delta n_e/n_0|$ is the density perturbation envelope ($\tilde{\eta}$ was measured in PIC simulations to be ~ 0.25 and varied weakly with density). This cancellation requires $\kappa' > 0$ (or $L > 0$), and thus for autoresonance to take place in the manner described, the density profile must increase in the direction of Langmuir wave (and pump wave) propagation.

3. SIMULATION RESULTS

We wish to determine the impact of $k_L \lambda_D$ on autoresonant growth. We define three density profiles, P1, P2 and P3, of the form $n_e = n_0[1 + (x - x_r)/L]$, where $x_r = 78 \mu\text{m}$ and the plasma length is $100 \mu\text{m}$. P1, P2 and P3 are characterised by $n_0/n_c = 0.05, 0.0425$ and 0.035 , respectively, giving for $L = \pm 100 \mu\text{m}$ ranges of $k_L \lambda_D$ across the plasma of $[0.26, 0.49]$, $[0.29, 0.54]$ and $[0.32, 0.60]$, where n_c is the usual critical density ($T_e = 1 \text{ keV}$ for all profiles).

In order to clearly identify a single Langmuir wave mode in PIC simulations, we choose a relatively strong pump (wavelength $\lambda_0 = 351 \text{ nm}$) of intensity $I_0 = 5 \times 10^{15} \text{ Wcm}^{-2}$ and seed of intensity $I_1 = 1 \times 10^{13} \text{ Wcm}^{-2}$ to drive the chosen mode significantly above the levels typically reached by laser interactions with the broadband noise in the plasma at early times (here defined as $t < 3 \text{ ps}$). The two lasers are initially resonant with a Langmuir wave at $x = x_r$ (in profile P2, $k_L \lambda_D = 0.37$ at $x = x_r$).

In Fig. 1A, the amplitude of the Langmuir wave envelope obtained by solving the 3-wave equations is shown for $L > 0$ (the case in which autoresonance is possible) in profile P2. The spatial growth of the Langmuir wave is observed to be along the parabola defined by Eq. (4), while the 3-wave phase mismatch is constant (Fig. 1B) over the autoresonant region. In Fig. 1C, the envelope amplitude of the Langmuir wave obtained from PIC simulations is shown, again using profile P2, while the corresponding

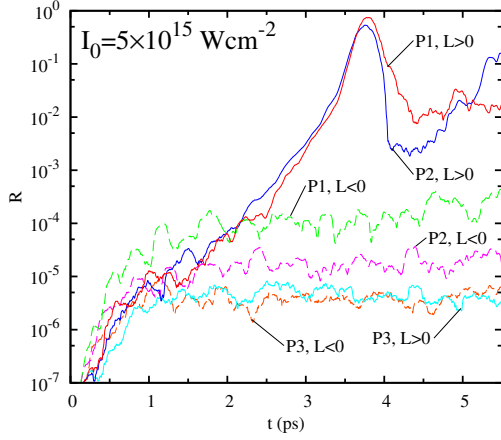


Figure 2. Smoothed reflectivity R as measured in various linear density profiles, obtained from PIC simulations.

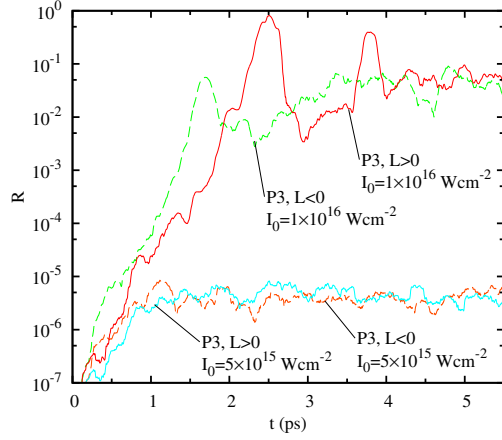


Figure 3. Smoothed reflectivity R as measured in density profile P3 with $I_0 = 5 \times 10^{15}$ and $I_0 = 1 \times 10^{16}$ Wcm^{-2} , obtained from PIC simulations.

3-wave phase mismatch is shown in Fig. 1D. The 3-wave model accurately predicts the local Langmuir wave amplitude and phase mismatch. We observe, therefore, that autoresonance is present in PIC simulations when a single Langmuir wave mode is driven by counter-propagating lasers. The Langmuir wave growth in simulations run using $L < 0$ is much reduced; consequently, the average reflectivity is greater in the $L > 0$ case by ~ 1.5 orders of magnitude. Very similar results are obtained when autoresonance is driven in profile P1 (at $x = x_r$ in P1, $k_L \lambda_D = 0.33$); the parabola defined in Eq. (4) depends only weakly on density, and the result is essentially unchanged.

We investigate now the behaviour of the reflectivity R when SRS grows *from noise only* (i.e. there is only one laser, I_0), and autoresonance may begin at all points in the plasma. In Fig. 2, R is shown for P1, P2 and P3, and for both $L > 0$ and $L < 0$ in each case. In P1 and P2, R is significantly greater when $L > 0$ compared to $L < 0$. Based on the observation of the behaviour of a single driven Langmuir wave mode discussed previously, we attribute this difference to autoresonance. In P3, there is no significant difference between the cases $L > 0$ and $L < 0$; in this case, the linear Landau damping is too great to allow the growth of SRS and thus does not permit the onset of a kinetic nonlinear frequency shift and autoresonant growth. In Fig. 3, the laser intensity is increased in P3. The growth and saturation of R is again similar for $L > 0$ and $L < 0$, but backscattering is now considerably beyond the levels predicted by Rosenbluth's amplification model. We conclude for this case that autoresonance is not the origin of this behaviour, but rather scattering from nonlinear plasma wave modes that are expected in the “strongly” kinetic regime with $k_L \lambda_D > 0.4$, as addressed in Refs. [13].

4. CONCLUSIONS

Autoresonance has been clearly observed in PIC simulations, where the growth of a driven autoresonant Langmuir wave mode matches closely in both amplitude and timing the predictions of a 3-wave coupling model. The reflectivity is observed to be significantly raised when the density gradient increases in the direction of Langmuir wave propagation, allowing autoresonant growth, compared to when the density gradient is of the opposing sign. This enhancement in reflectivity is observed both when a single Langmuir wave mode is preferentially driven using counter-propagating lasers, and when only a single laser is applied. The autoresonant growth rate depends only weakly on density until a cut-off at high values of $k_L \lambda_D$.

Good agreement between a 3-wave model with a kinetic nonlinear frequency shift and PIC simulations has been found at values of $k_L \lambda_D$ up to 0.37, suggesting the nonlinear frequency shift and consequently autoresonance are applicable beyond the regime typically referred to as “weakly kinetic”.

References

- [1] V. V. Gorgadze, L. Frièdland, and J. S. Wurtele, *Phys. Plasmas* **14**, 082317 (2007)
- [2] G. B. Andresen *et al.*, *Phys. Rev. Lett.* **106**, 025002 (2011)
- [3] C. S. Liu, M. N. Rosenbluth, and R. B. White, *Phys. Rev. Lett.* **31**, 697 (1973)
- [4] M. N. Rosenbluth, *Phys. Rev. Lett.* **29**, 565 (1972)
- [5] G. J. Morales and T. M. O’Neil, *Phys. Rev. Lett.* **28**, 417 (1972)
- [6] T. M. O’Neil, *Phys. Fluids* **8**, 2255 (1965)
- [7] H. X. Vu, D. F. DuBois, and B. Bezzerides, *Phys. Plasmas* **9**, 1745 (2002); *Phys. Plasmas* **14**, 012702 (2007)
- [8] J. L. Kline *et al.*, *Phys. Rev. Lett.* **94**, 175003 (2005); *Phys. Plasmas* **13**, 055906 (2006)
- [9] P. E. Masson-Laborde *et al.*, *Phys. Plasmas* **17**, 092704 (2010)
- [10] T. Chapman *et al.*, *Phys. Rev. Lett.* **108**, 145003 (2012)
- [11] O. Yaakobi and L. Frièdland, *Phys. Plasmas* **15**, 102104 (2008)
- [12] T. Chapman *et al.*, *Phys. Plasmas* **17**, 122317 (2010)
- [13] D. A. Russell and H. A. Rose, *Phys. Plasmas* **8**, 4784 (2001); D. S. Montgomery *et al.*, *Phys. Rev. Lett.* **87**, 155001 (2001); D. Bénisti, D. J. Strozzi, and L. Gremillet, *Phys. Plasmas* **15**, 030701 (2008); B. Afeyan *et al.*, *Proc. IFSA (Inertial Fusion Sciences and Applications 2003, Monterey, CA)*, edited by B. Hammel *et al.*, American Nuclear Society, 213 (2004)